## Supplementary Information for:

# Evidence for a Large-Scale Brain System Supporting Allostasis and Interoception in Humans

**Authors:** Ian R. Kleckner[1*], Jiahe Zhang[1], Alexandra Touroutoglou[2,3,4], Lorena Chanes[1,3,4], Chenjie Xia[3,5], W. Kyle Simmons[6,7], Karen S. Quigley[8,1], Bradford C. Dickerson[3,5‡], Lisa Feldman Barrett[1,3,4*‡]

**Affiliations:**

[1]Department of Psychology, Northeastern University, Boston, MA.

[2]Department of Neurology, Massachusetts General Hospital and Harvard Medical School

[3]Athinoula A. Martinos Center for Biomedical Imaging

[4]Psychiatric Neuroimaging Division, Department of Psychiatry, Massachusetts General Hospital and Harvard Medical School, Charlestown, MA

[5]Frontotemporal Disorders Unit, Department of Neurology, Massachusetts General Hospital and Harvard Medical School, Charlestown, MA

[6]Laureate Institute for Brain Research, Tulsa, OK

[7]School of Community Medicine, The University of Tulsa, Tulsa, OK

[8]Edith Nourse Rogers Memorial VA Hospital, Bedford, MA

[*]Corresponding authors: ian_kleckner@urmc.rochester.edu, l.barrett@neu.edu

[‡]Shared senior authorship

.

## Supplementary Discussion

**Detailed description of subcortical, hippocampal, brainstem, and cerebellar connectivity within the interoceptive system.** Here, we briefly justify the inclusion of each non-cortical region in our connectivity analyses, report its observed intrinsic connectivity patterns with the allostatic/interoceptive system seeds (Fig. 4 and Supplementary Figure 6), and compare our results with published tract-tracing studies showing monosynaptic anatomical connectivity among these regions (Table 2). Discrepancies between our results and tract-tracing are only indicated if our fMRI results failed to show connectivity between regions that are monosynaptically connected. fMRI intrinsic connectivity reflects both direct and indirect (multisynaptic) connections[46,47] and thus our results sometimes show connectivity for regions that are disynaptically connected.

**Thalamus.** We examined connectivity to two thalamic nuclei: the posterior part of the ventromedial nucleus (VMpo; for a review, see [1]) for interoceptive input specifically and the larger ventral posterior (VP) complex for somatic input more broadly[2]. Our fMRI results revealed that all cortical and amygdalar seeds exhibited connectivity with the VMpo and VP. This is entirely consistent with tract-tracing studies showing direct projections of VMpo or VP to dpIns, dmIns, and dorsal ACC/aMCC (for a review, see [1]). Our other cortical and amygdalar seeds have multisynaptic connectivity to VMpo and VP by way of aMCC.

**Hypothalamus.** The hypothalamus is a critical region for allostatic regulation of the body; the paraventricular nucleus in the medial zone is particularly responsible for visceromotor control of autonomic, endocrine, and immune function[3]. Our review of tract tracing studies clearly indicated connectivity from each cortical and amygdalar seed except with dpIns, despite

evidence from tract-tracing, and with lvaIns to the hypothalamus (which was not predicted) [4-10]. The lack of functional connectivity between lvaIns and the hypothalamus is not surprising because the lateral portion of the ventral anterior insula is part of a sensory integration network in orbitofrontal cortex in monkeys and humans[4,10] that has little connection to the hypothalamus, except for light connections to the posterior lateral hypothalamus at the level of the mammillary bodies[4]. We were unable to identify the expected connectivity between the dAmy and any part of the hypothalamus.

**Cerebellum.** The cerebellum is a key structure in sensorimotor regulation because it sends efferent copies (i.e., predictions) to the cortex to help the brain distinguish between the anticipated sensory consequences of self-initiated by the body vs. those that are unexpected[11,12]. All cortical seeds and the dAmy seed exhibited connectivity with the cerebellum. More specifically, all seeds exhibited connectivity to lobules IV, V, VI and VIIIB, consistent with the cerebellar "somatosensory" network. The default mode portion of the interoceptive system is additionally connected to lobule IX and Crus I, whereas the salience portion of system is additionally connected to lobule VIIIA (for a specific parcellation of cerebellar intrinsic connectivity, see [13]).

**Amygdala.** The amygdala is a key subcortical region for both interoceptive input (via its lateral nucleus) and visceromotor control (via its central nucleus)[14], and is part of both the salience and the default mode networks[15,16]. All of our cortical seeds exhibited connectivity to the amygdala seed except for the pACC seed, which had limited connectivity to the left amygdala (only the dorsal section, which contains the central nucleus). This is consistent with results from tract-tracing studies, which show that each of our cortical seeds projects monosynaptically to the dorsal amygdala[5,17-21].

**Hippocampus.** The hippocampus is a key subcortical hub in the default mode network[16] that is strongly connected to the amygdala (for a review, see [22]). Our fMRI results showed that all cortical seeds and the dAmy seed exhibited connectivity to the entire hippocampus except for the aMCC seed, which exhibited connectivity to only the posterior hippocampus, and the dmIns seed, which exhibited connectivity only to the anterior and posterior hippocampus. Our results are consistent with tract-tracing studies indicating direct projections from the amygdala to the hippocampus and indirect projections from many regions of the cortex to the hippocampus; specifically, vaIns, sgACC, pACC, and aMCC all project to the entorhinal cortex, which projects to the hippocampus (for a review, see [22]). Other cortical regions such as the aMCC and dmIns can connect to the hippocampus in three steps: first to a cortical hub (e.g., vaIns), then to and the entorhinal cortex, then to the hippocampus.

**Ventral striatum.** The striatum is a subcortical region in the basal ganglia comprising the caudate, putamen, and nucleus accumbens, and its ventral portion is important for controlling inhibitory signals to brainstem visceromotor targets[23,24]. Specifically, cortical regions send excitatory (glutamatergic) signals to the striatum, which enhance inhibition of brainstem visceromotor targets; these connections also have the capacity to release visceromotor targets from tonic inhibition via striatal connections to the pallidum[24]. All of our cortical and amygdalar seeds exhibited connectivity to the ventral striatum, except for dmIns, which exhibited connectivity to a portion of the ventral striatum. This is consistent with tract-tracing studies showing monosynaptic connections from each of our seeds to the ventral striatum[7,25-29].

**Periaqueductal gray (PAG).** The PAG is a midbrain nucleus important visceromotor control[30]. It is difficult to precisely localize using 3-T scanning procedures because it encircles the cerebral aqueduct (e.g., [31]). Nonetheless, the results of our intrinsic connectivity analysis

largely mirror those for the hypothalamus. The tract-tracing literature has identified monosynaptic connectivity to the PAG from all seeds[60,121] except the dmIns and dpIns[32], and the lvaIns[32]. All cortical visceromotor seeds demonstrated the expected connections with the PAG: aMCC, pACC, and sgACC. We did not observe the expected connectivity with the mvaIns nor with the dAmy. As expected, connectivity with the lvaIns and dpIns was not observed.

**Parabrachial nucleus (PBN).** The PBN is a nucleus in the pons that relays interoceptive input from the body to the brain[1] and also serves visceromotor functions[33]. All cortical seeds and the dAmy seed exhibited connectivity with the PBN. This is in agreement with the tract-tracing literature showing monosynaptic connectivity to the PBN from each of our seeds[7,26,27,34,35] except for the aMCC[36], which must first project to another cortical hub (e.g., vaIns) before projecting to the PBN.

**Nucleus of the solitary tract (NTS).** The NTS is a key relay nucleus in the medulla that is on a cranial interoceptive pathway from the viscera to the brain[12,13,22,23] and also contributes to visceromotor control[1,33,37-39]. We observed NTS connectivity with the dAmy seed and with all cortical seeds except for the sgACC. This is largely consistent with the tract-tracing literature showing monosynaptic projections to the NTS from each of our seeds[27,35,40,41]. Failure to observe the sgACC connection is perhaps due to the small size of the sgACC and increased noise due to partial-volume effects of the nearby white matter in the corpus callosum.

**Laboratory validation of the allostatic/interoceptive system in humans.** The following text details our findings of the association between connectivity in the allostatic/interoceptive system in humans and an index of interoception: the concordance between objective and subjective measures of bodily arousal. We measured sympathetic nervous

system arousal using skin conductance responses (SCRs)[42] while participants viewed each photo for six seconds. We selected SCRs as an index of sympathetic nervous system activity because, although effects from SCRs specifically might not ascend to interoceptive brain systems, the simultaneous non-SCR effects of sympathetic nervous system activity likely are processed through interoceptive pathways. After each image, participants reported their subjective experience of arousal using a validated self-report scale[43]. Using multi-level regression procedure to account for the nested and repeated-measures design of this experiment (for a review, see [44]), we found that the number of SCRs in response a picture (either 0, 1, 2, 3, or 4 SCRs to a given picture) predicted the intensity of arousal experiences in response to the same picture across all participants and pictures ($B = 0.21$, $p < 0.001$), consistent with prior research (e.g., [45]). Furthermore, as predicted, individuals with stronger intrinsic connectivity between primary interoceptive cortex (dpIns) and the aMCC had a stronger correspondence between sympathetic arousal and subjective experience of arousal than did those with weaker connectivity (regression $B = 0.56$; $p < 0.003$; Supplementary Figure 8). We focused on the aMCC because it was an a priori visceromotor seed region (Table 1), a connector hub[46], and consistently replicated tract-tracing connectivity to non-cortical allostatic nuclei. For completeness, our results focused on the number of SCRs in response to each image and we did not find analogous results using the amplitude of SCRs in response to each image.

**Reconciling prior studies that reported a negative correlation between default mode and salience network activity.** Many studies have found that the default mode and salience networks have task-related activity that is negatively correlated (i.e., when the BOLD signal in one network goes up, the BOLD signal in the other network goes down). Such findings are often interpreted as evidence that the brain has either an internal focus on an external focus. This

inverse relationship is often the consequence of removing the mean signal change from all voxels in each volume before proceeding with data analysis (called "global-signal regression"; e.g., [47]). A more reasonable interpretation, however, may be that when one network increases its neural activity compared to some baseline, the other might show a relative decrease in activity from that baseline (which does not mean that network is irrelevant to the task at hand). Alternatively, one network might show a smaller increase than the other (which, when mean signal change is removed, would appear as a negative relationship between the two networks).

**Supplementary Tables**

**Supplementary Table 1.** Functional connectivity between interoceptive and visceromotor regions in humans.

| Seed | Target | Connectivity (Pearson's *r*) Mean ± SD | *t*-statistic | *p*-value[a] |
|---|---|---|---|---|
| dpIns | aMCC | 0.11 ± 0.16 | 11.21 | $3.5\times10^{-24}$ |
| dpIns | dAmy | 0.15 ± 0.16 | 16.02 | $5.2\times10^{-41}$ |
| dpIns | dmIns | 0.17 ± 0.17 | 17.34 | $9.9\times10^{-46}$ |
| dpIns | mvaIns | 0.10 ± 0.16 | 10.87 | $4.6\times10^{-23}$ |
| dpIns | lvaIns | 0.14 ± 0.17 | 13.33 | $1.8\times10^{-31}$ |
| dpIns | pACC | 0.06 ± 0.16 | 5.81 | $1.8\times10^{-8}$ |
| dpIns | sgACC | 0.07 ± 0.15 | 7.74 | $2.1\times10^{-13}$ |
| | | | | |
| dmIns | aMCC | 0.25 ± 0.17 | 23.66 | $1.1\times10^{-67}$ |
| dmIns | dAmy | 0.16 ± 0.17 | 15.91 | $1.3\times10^{-40}$ |
| dmIns | mvaIns | 0.10 ± 0.16 | 10.51 | $7.0\times10^{-22}$ |
| dmIns | lvaIns | 0.08 ± 0.17 | 7.86 | $9.5\times10^{-14}$ |
| dmIns | pACC | -0.02 ± 0.19 | -1.42 | $1.6\times10^{-1}$ |
| dmIns | sgACC | -0.09 ± 0.17 | -8.36 | $3.4\times10^{-15}$ |

*Note:* [a]p-values from one-sample two-tailed t-test to assess whether connectivity is non-zero, $N = 280$ (discovery sample).

**Supplementary Table 2.** Correspondence between networks in the interoceptive system and established resting state networks in humans.

| **Percent of networks 1 and 2 in each established resting state network** | | | |
|---|---|---|---|
| | | Default mode network | Salience network |
| Network 1 | Discovery | **63%** | 15% |
| | Replication | **75%** | 15% |
| Network 2 | Discovery | 7% | **60%** |
| | Replication | 6% | **57%** |
| **Percent of each established resting state network in networks 1 and 2** | | | |
| | | Default mode network | Salience network |
| Network 1 | Discovery | **77%** | 14% |
| | Replication | **86%** | 14% |
| Network 2 | Discovery | 9% | **65%** |
| | Replication | 9% | **64%** |

*Note:* The percent in each cell indicates the fraction of the brain map in the row that overlaps with the brain map in the column. The top part of the table shows that the majority of Network 1 overlaps with the default mode network and the majority of Network 2 overlaps with the salience network. The bottom part of the table shows that the majority of the default mode network overlaps with Network 1 and the majority of the salience network overlaps with Network 2.

Calculations of networks 1 and 2 were performed at the threshold shown in Fig. 3 ($p < 10^{-5}$ uncorrected using $N = 280$). The default mode and the salience networks were defined based on default mode and ventral attention networks from Yeo, et al.[48] at a threshold of $z(r) > 0.05$ where z is the Fisher's z transformation.

**Supplementary Table 3.** Anatomical connections from the interoceptive system to visceromotor control regions (hypothalamus or PAG).

| | Cortical region | To hypothalamus | To PAG |
|---|---|---|---|
| **Default Mode Network Only** | From ventromedial prefrontal cortex (BA 12) | Yes | Yes |
| | From medial orbitofrontal cortex (BA 11, 13) | Yes | No |
| | From dorsomedial prefrontal cortex (BA 9, 10) | Yes | Yes |
| | From posterior cingulate cortex (BA 23, 31) | No | BA 23ab but not BA 31 |
| | From ventral precuneus (BA 7) | No | No |
| | From angular gyrus (BA 39) | No | No |
| | From middle frontal gyrus (BA 46) | Yes | Yes |
| **Salience Network Only** | From dorsal precuneus (BA 5) | No | No |
| | From medial frontal gyrus (BA 6) | Yes | No |
| | From fusiform gyrus (BA 37) | No | No |
| | From middle temporal gyrus (BA 21) | No | Yes |
| | From precentral gyrus (BA 6) | Yes | Yes |
| **Hubs Connecting Networks Default Mode and Salience Networks** | From midcingulate cortex (BA 31) | Yes | Yes |
| | From medial postcentral gyrus (BA 6) | No | No |
| | From parahippocampal gyrus (BA 30) | No | No |
| | From inferior temporal gyrus (BA 36) | No | No |
| | From cuneus (BA 30) | No | No |
| | From superior temporal sulcus (BA 13, 22) | No | Yes |
| | From temporal pole (BA 38) | No | No |
| | From inferior frontal gyrus (BA 47) | Yes | Yes |

*Note:* Each cell shows the citation number for the paper indicating tract-tracing results in monkey (or sometimes in rat [49]). Hypothalamus projections obtained from references [4,49]; PAG projections obtained from references [30,32,50,51]. We only assessed projections from cortical regions to the hypothalamus or PAG (not from hypothalamus or PAG to cortical) because we wanted to assess if these cortical regions support visceromotor control.
PAG = periaqueductal gray.

**Supplementary Table 4.** Connector hubs within the interoceptive system.

| Cluster | Volume ($mm^3$) | MNI Center of Mass (mm) | | | Brodmann Area | Anatomic Name | Rich Club Hub | Visceromotor |
|---|---|---|---|---|---|---|---|---|
| | | X | Y | Z | | | | |
| 1 | 3712 | 45 | -21 | 11 | Near BA 13, 41 | Dorsal posterior insula | No | Yes (e.g., hypothalamus in rat[8], PBN in rat[34]) |
| 2 | 2136 | 24 | 17 | -17 | Near BA 47 | Ventral anterior insula<br>Inferior frontal gyrus | Yes | Yes (e.g., hypothalamus[4]; PAG[32]) |
| 3 | 1224 | 49 | 28 | -4 | Near BA 47 | Inferior frontal gyrus | No | Yes (e.g., PAG[32]) |
| 4 | 952 | 28 | -4 | -35 | Near BA 36 | Inferior temporal gyrus | No | Apparently no |
| 5 | 648 | 19 | -46 | 3 | Near BA 30 | Parahippocampal gyrus | Yes | Apparently no |
| 6 | 536 | 4 | -2 | 36 | BA 24 | Anterior midcingulate cortex<br>Posterior midcingulate cortex | Yes | Yes (e.g., hypothalamus[4], PAG[32]) |
| 7 | 368 | 53 | -41 | 6 | Near BA 22 | Superior temporal sulcus | No | Yes (e.g., PAG[51]) |
| 8 | 320 | 53 | -45 | 20 | BA 13 | Superior temporal sulcus | No | Yes (e.g., PAG[32]) |
| 9 | 304 | 54 | 15 | -13 | BA 22 | Superior temporal sulcus | Yes | Yes (e.g., PAG[51]) |
| 10 | 264 | 38 | 7 | -39 | BA 38 | Temporal pole | No | Apparently no |
| 11 | 256 | 11 | -63 | 16 | Near BA 30 | Cuneus<br>Medial occipital | Yes | Apparently no |
| 12 | 208 | 7 | -23 | 49 | Near BA 31, 6 | Midcingulate cortex<br>Postcentral gyrus | Yes | Yes (e.g., hypothalamus[4]; PAG[32]) |

*Note.* This table shows clusters from the overlap of two networks displayed in Fig. 3. One of the superior temporal sulcus clusters (7, 8, and 9) is not easily visible in Fig. 3. Clusters are ordered from largest to smallest. "Near" = within 3 mm. To assess whether a cluster was visceromotor, we reviewed the monkey tract-tracing literature for evidence of a monosynaptic anatomical projection to the following subcortical and brainstem visceromotor regions: hypothalamus, periaqueductal gray, parabrachial nucleus, ventral striatum, and nucleus of the solitary tract. We indicated "Yes" if we found evidence of projections to any of those subcortical and brainstem regions and we indicated "No" if we found no evidence of any of those projections using references [4,30,32,34,51,52].

NTS = nucleus of the solitary tract; PAG = periaqueductal gray; PB = parabrachial nucleus; VS = ventral striatum.

**Supplementary Table 5.** International affective picture system (IAPS) images used in the evocative pictures task.

| Unpleasant High arousal | Unpleasant Low arousal | Neutral Low arousal | Pleasant High arousal | Pleasant Low arousal |
|---|---|---|---|---|
| 3001 | 2039 | 1122 | 4660 | 1441 |
| 3010 | 2101 | 2038 | 4664 | 1601 |
| 3053 | 2104 | 2214 | 4668 | 1604 |
| 3080 | 2221 | 2377 | 4698 | 1610 |
| 3102 | 2271 | 2381 | 5621 | 1620 |
| 3110 | 2525 | 2385 | 5629 | 2299 |
| 3120 | 2722 | 2411 | 5950 | 2304 |
| 3266 | 4233 | 2485 | 8030 | 2370 |
| 3530 | 5130 | 2487 | 8080 | 2388 |
| 6313 | 6010 | 2495 | 8163 | 2530 |
| 6520 | 7011 | 2514 | 8179 | 2540 |
| 9163 | 7060 | 2518 | 8180 | 2560 |
| 9412 | 7078 | 2575 | 8186 | 2598 |
| 9413 | 7234 | 2870 | 8370 | 5891 |
| 9635 | 7290 | 5395 | 8492 | 7325 |
| | | 5510 | | |
| | | 5531 | | |
| | | 5731 | | |
| | | 6150 | | |
| | | 7000 | | |
| | | 7003 | | |
| | | 7004 | | |
| | | 7021 | | |
| | | 7056 | | |
| | | 7077 | | |
| | | 7080 | | |
| | | 7207 | | |
| | | 7503 | | |
| | | 7550 | | |
| | | 7700 | | |

*Note*. Pictures are ordered by IAPS number. The experimental picture order was block-randomized (see Methods: Procedure). Normative ratings for IAPS pictures have been reported elsewhere[53].

**Supplementary Figures**

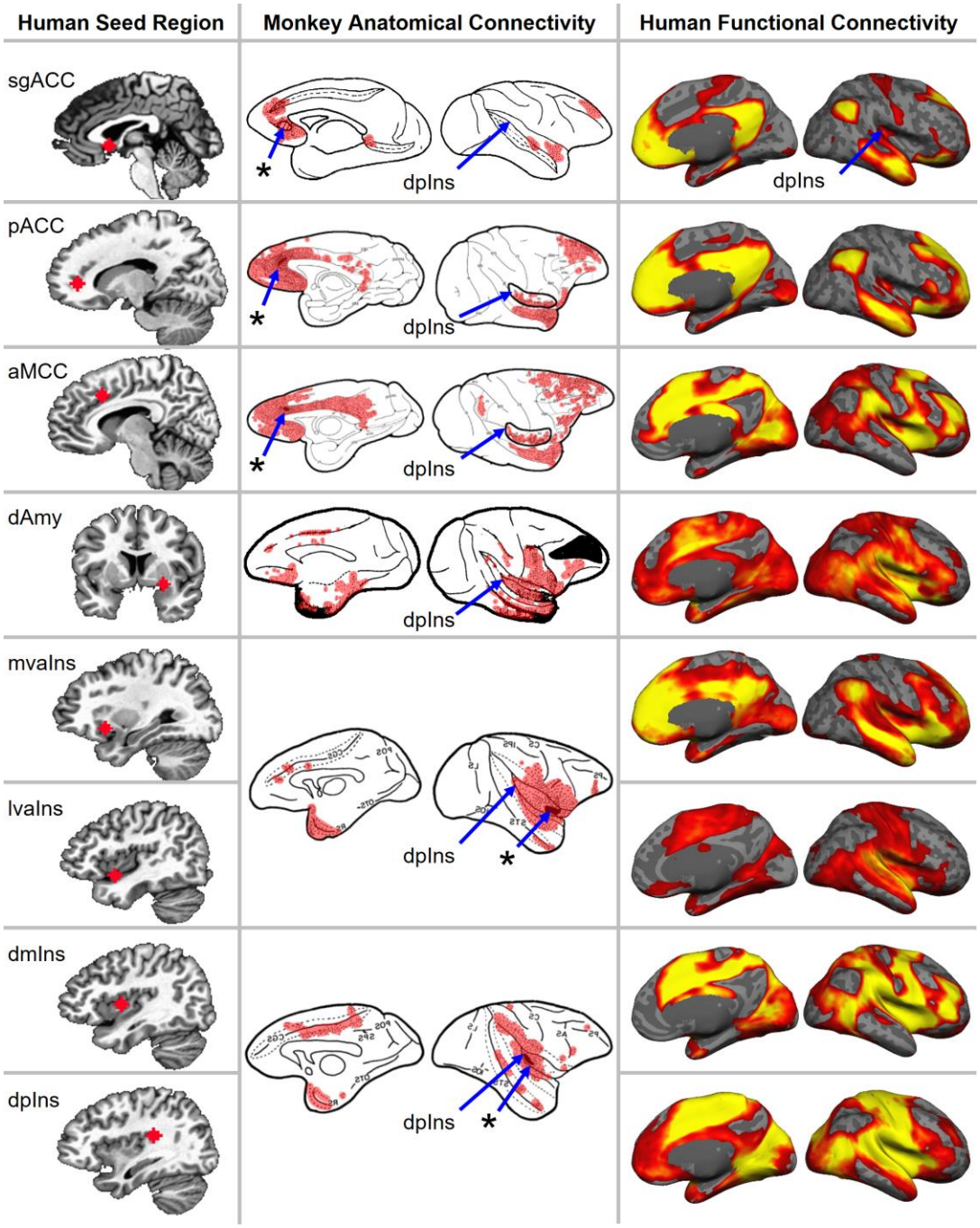


**Supplementary Figure 1.** Replication of the interoceptive system connecting the cortical and amygdalar visceromotor regions and primary interoceptive regions shown in Fig. 2 using the replication sample ($N$ = 270). The color map ranges from $p = 10^{-5}$ in red to $p = 10^{-40}$ in yellow, uncorrected and on a log scale.

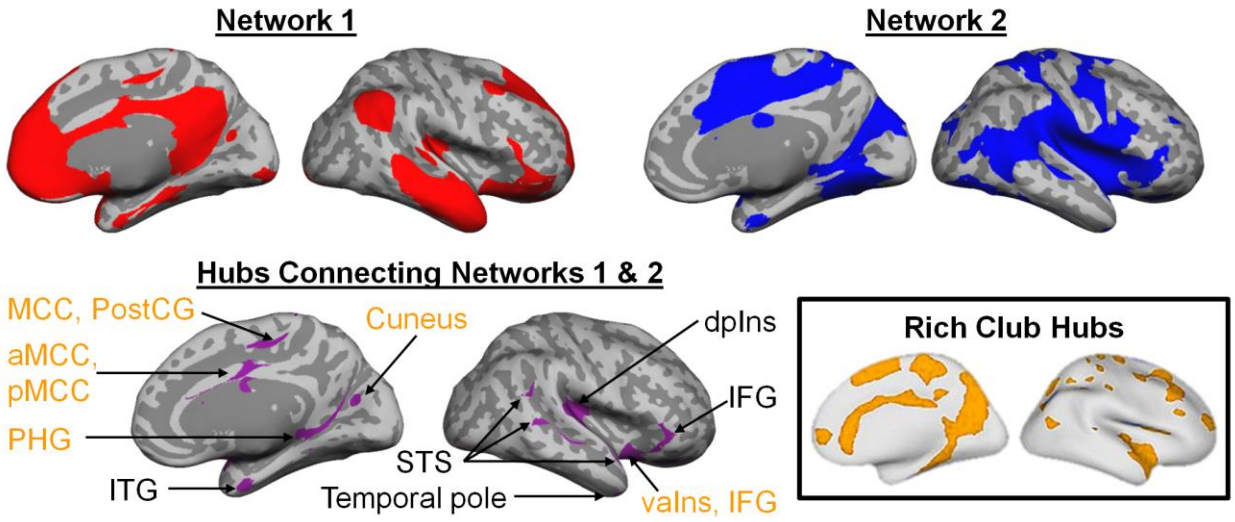


**Supplementary Figure 2.** Replication of the interoceptive system shown in Fig. 3 using the replication sample ($N$ = 270). Intrinsic connectivity maps binarized at $p < 10^{-5}$ uncorrected. Rich club hubs figure adapted with permission from van den Heuval & Sporns (2013)[54].

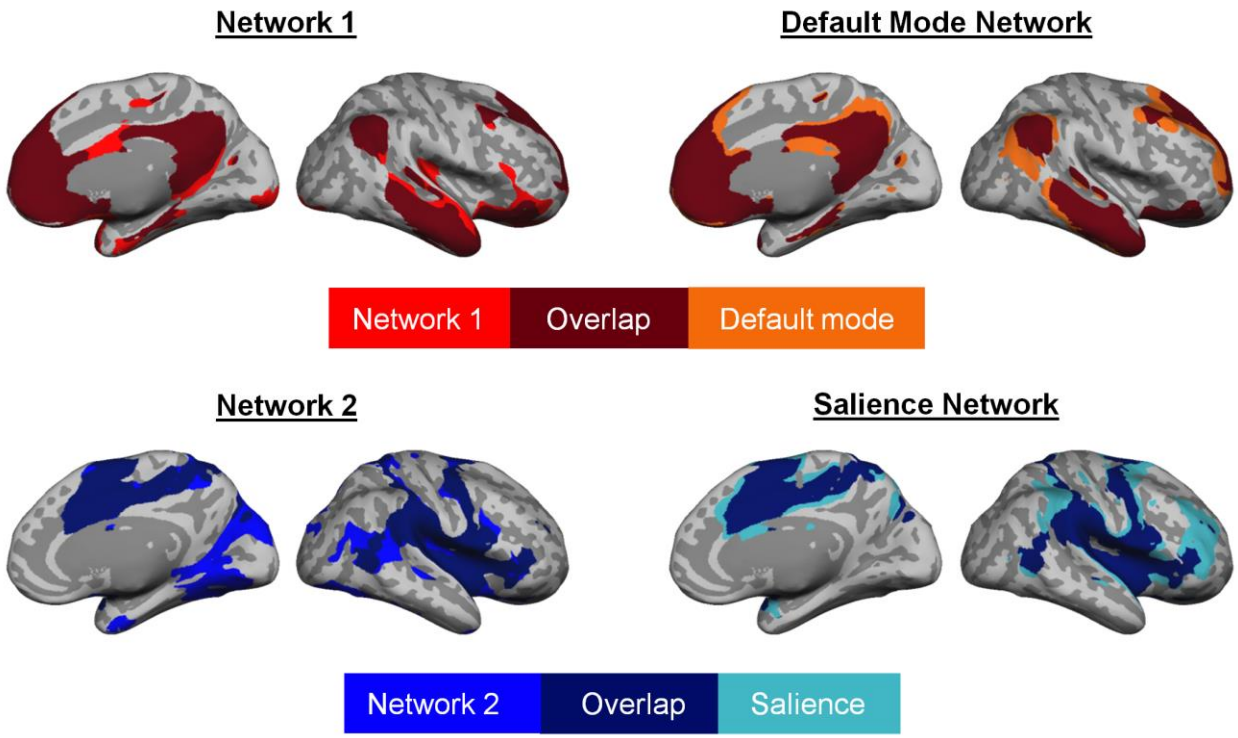


**Supplementary Figure 3**. Correspondence between allostatic/interoceptive system networks (binarized at $p < 10^{-5}$ uncorrected) and established default mode and salience networks in the discovery sample ($N = 280$). The masks of the established networks were computed based on Yeo et al. (2011)[48] using a traditional volume-based approach[55,56] on a sample of 150 subjects (see Methods for description of subjects). The correspondence between the interoceptive system networks and established networks was replicated in a second sample of $N = 270$ (Supplementary Figure 4).

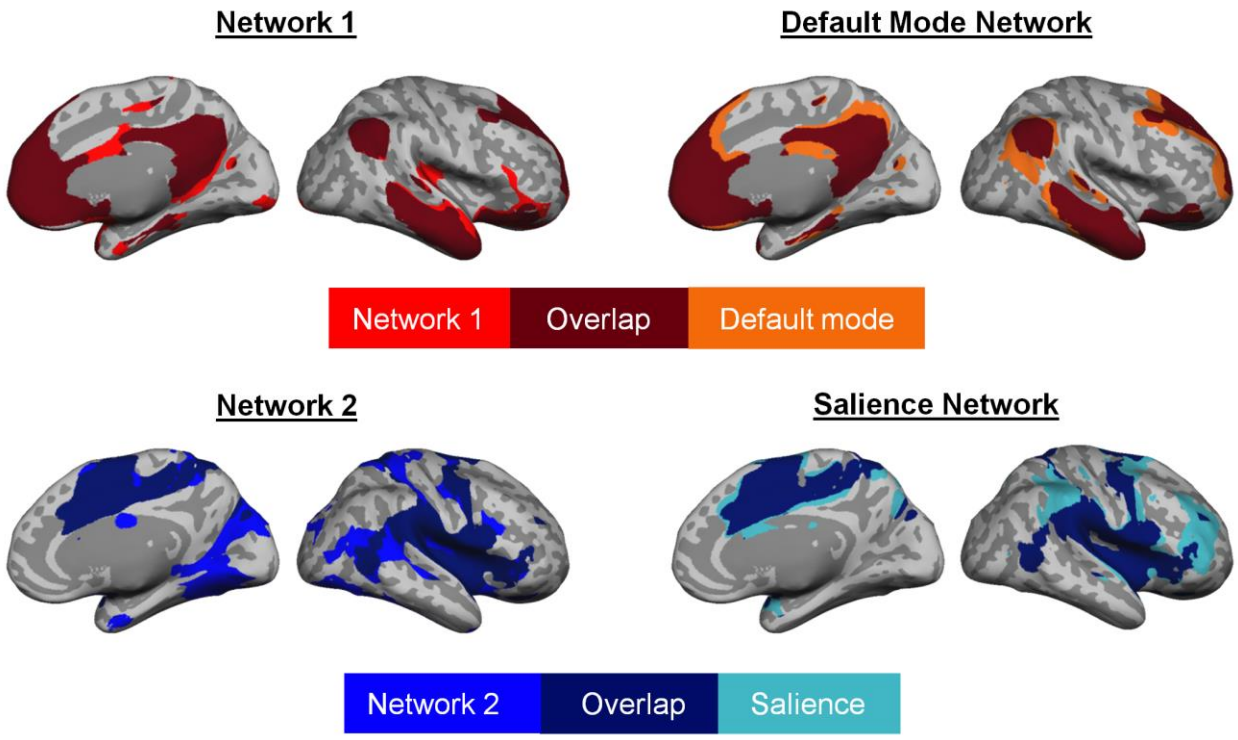


**Supplementary Figure 4.** Replication of correspondence between interoceptive system networks (binarized at $p < 10^{-5}$ uncorrected) and established default mode and salience networks shown in Supplementary Figure 3 using the replication sample ($N = 270$). The masks of the established networks were computed based on Yeo et al.[48] using a traditional volume-based approach[55,56] on a sample of 150 subjects (see Methods for description of subjects).

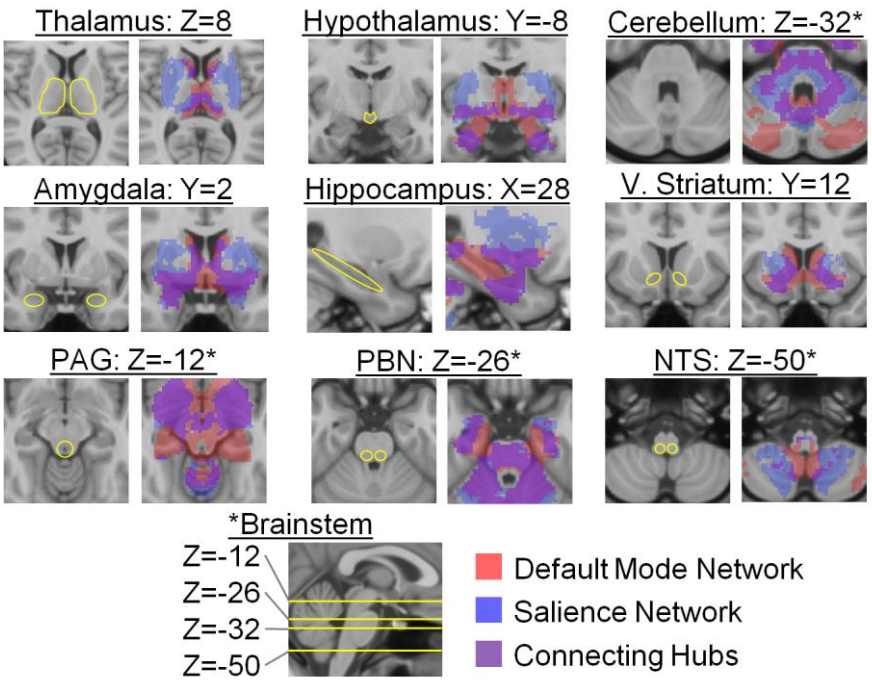


**Supplementary Figure 5.** Replication of subcortical connectivity of the two intrinsic networks within the interoceptive system in Fig. 4 using the replication sample ($N$ = 270; $p < 10^{-5}$ uncorrected, one-sample two-tailed t-test). PAG = periaqueductal gray; PBN = parabrachial nucleus; V. Striatum = ventral striatum; NTS = nucleus of the solitary tract.

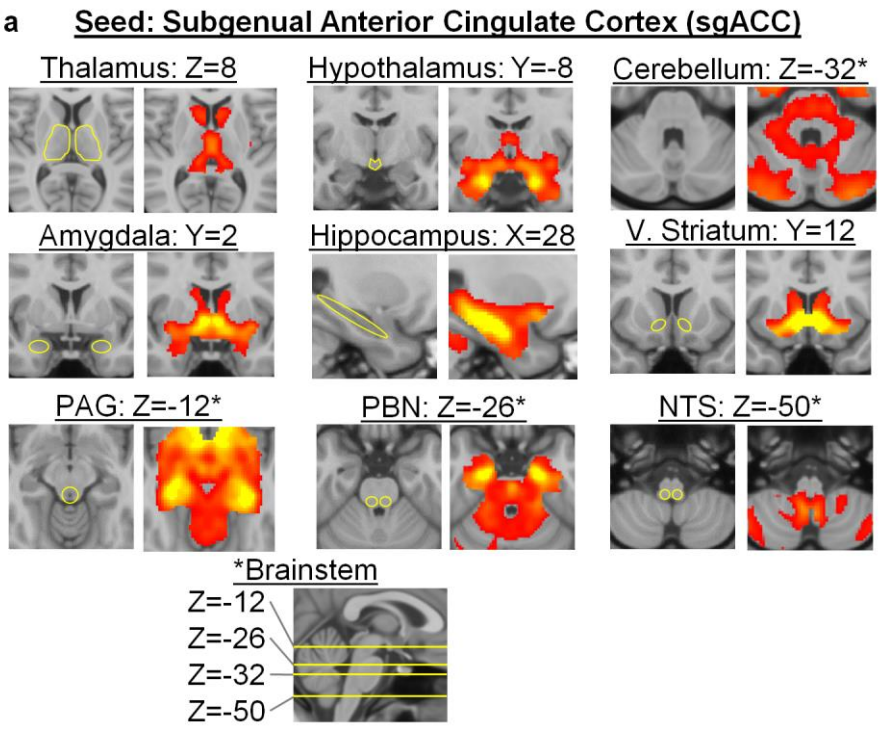


**Supplementary Figure 6.** Subcortical connectivity of each of the eight cortical and amygdalar seeds used to delineate the interoceptive system using the discovery sample ($N$ = 280). The color scale ranges from $p = 0.05$ in red to $p = 10^{-50}$ in yellow, uncorrected and on a log scale. (a) Seed at subgenual anterior cingulate cortex (sgACC). (b) Seed at pregenual anterior cingulate cortex (pACC). (c) Seed at anterior midcingulate cortex (aMCC). (d) Seed at dorsal amygdala (dAmy). (e) Seed at medial ventral anterior insula (mvaIns). (f) Seed at lateral ventral anterior insula (lvaIns). (g) Seed at dorsal mid insula (dmIns). (h) Seed at dorsal posterior insula (dpIns). PAG = periaqueductal gray; PBN = parabrachial nucleus; V. Striatum = ventral striatum; NTS = nucleus of the solitary tract.

**Supplementary Figure 6** continued

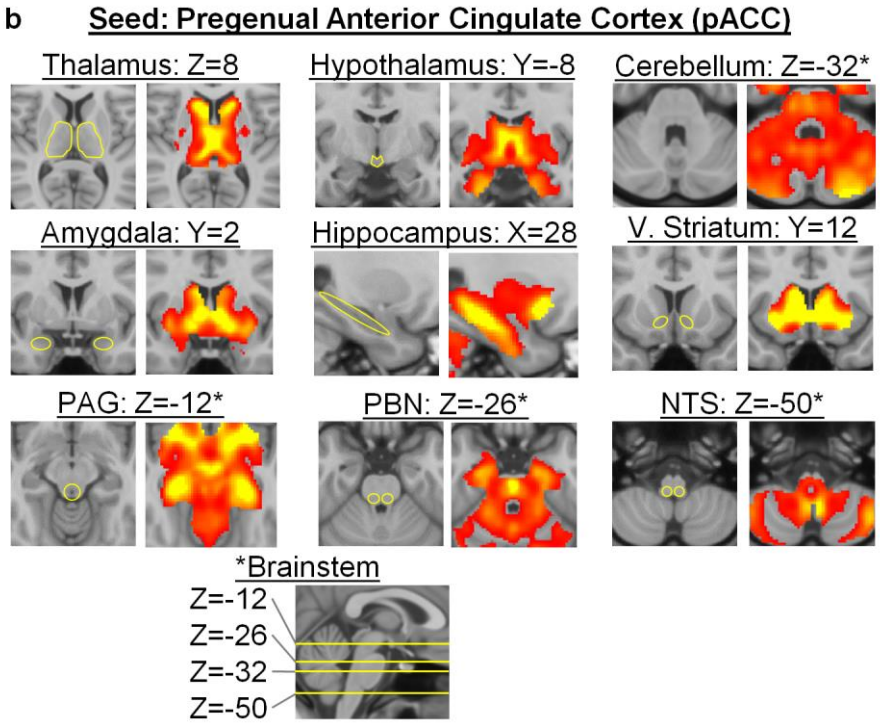


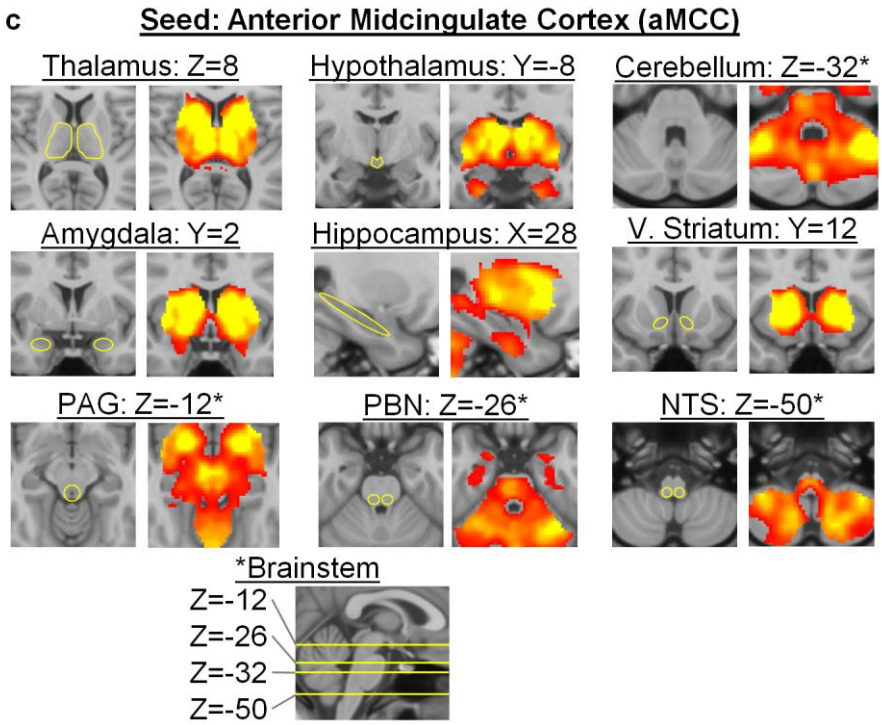

**Supplementary Figure 6** continued

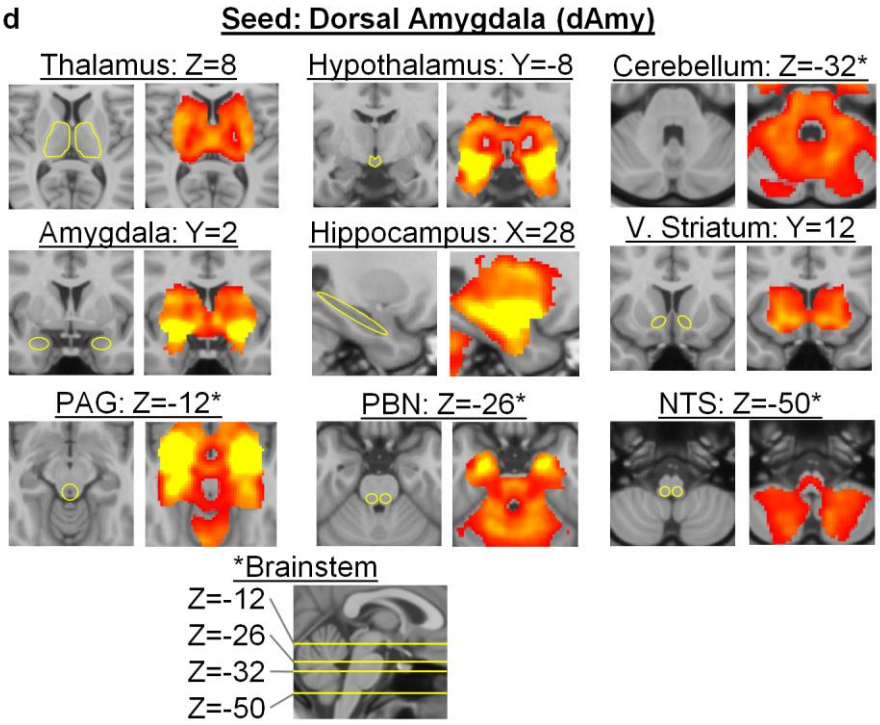


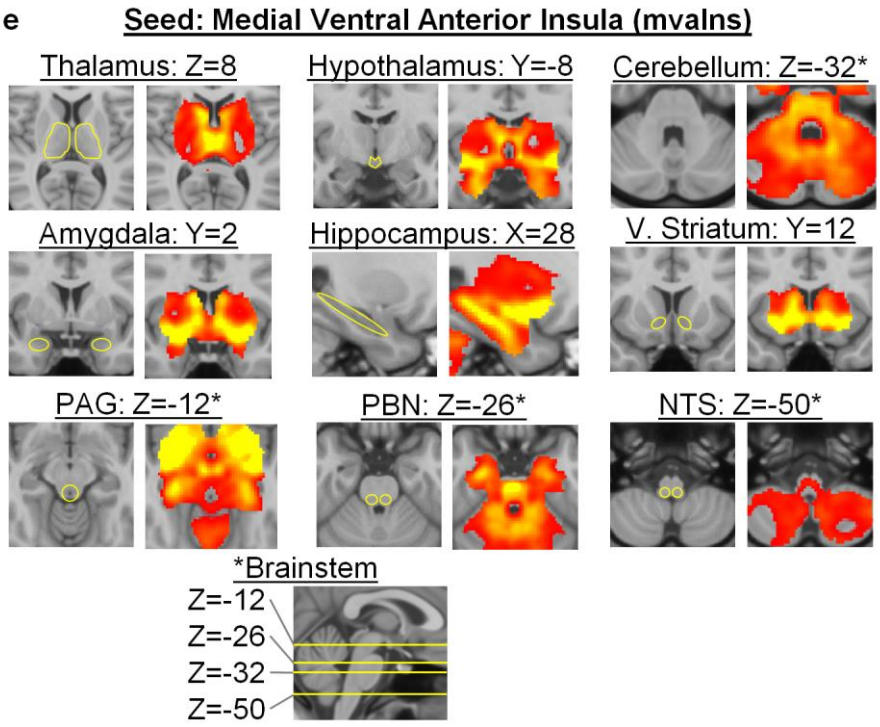

**Supplementary Figure 6** continued

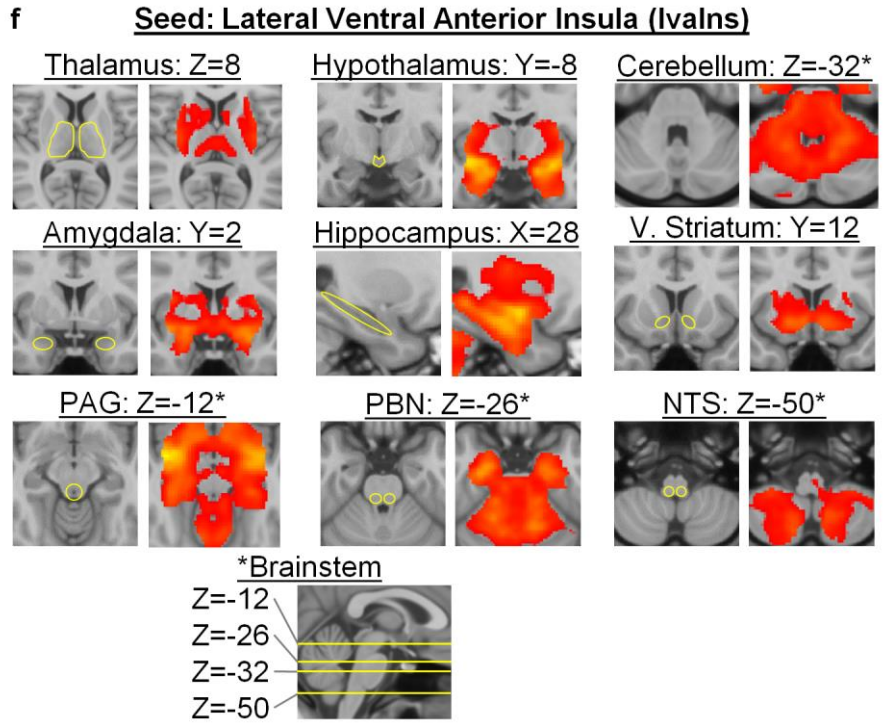


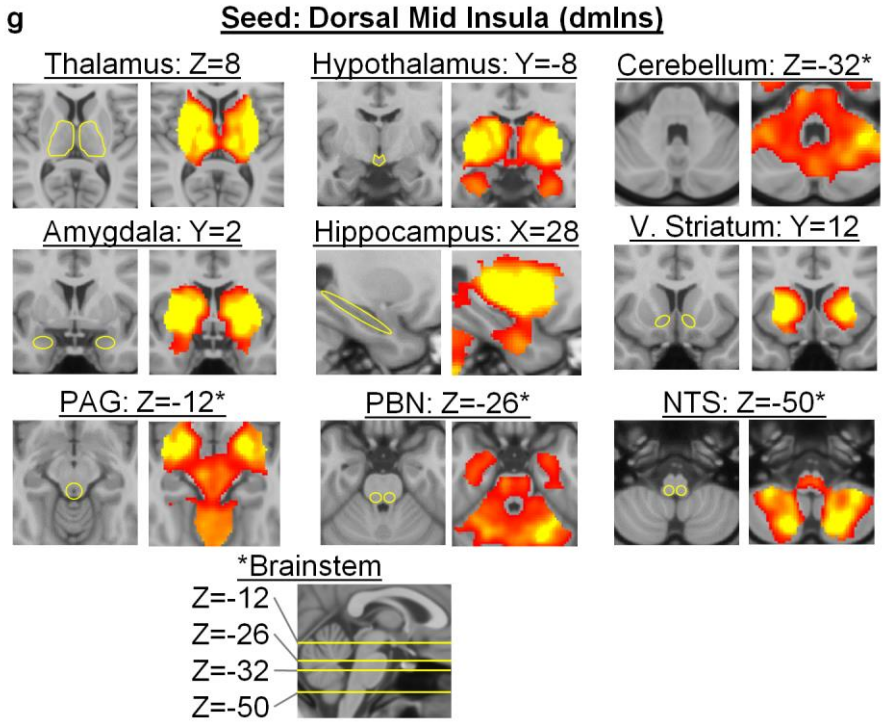

**Supplementary Figure 6** continued

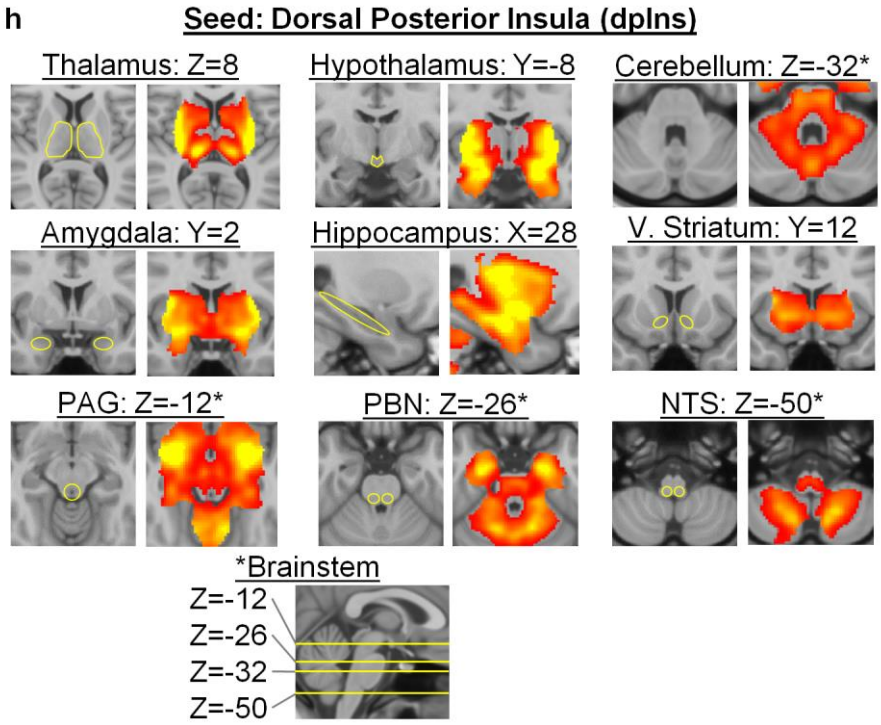

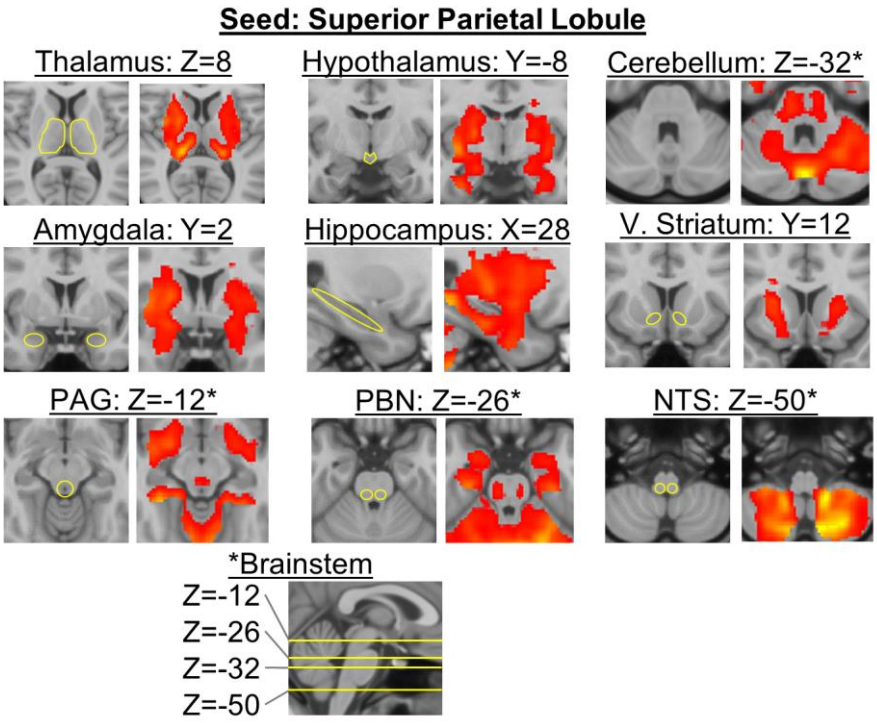


**Supplementary Figure 7.** Subcortical connectivity of the superior parietal lobule does not involve non-cortical targets important for allostasis (hypothalamus, PAG, PBN, NTS), suggesting a degree of specificity in the functional connections between cortical regions in the allostatic/interoceptive system and subcortical regions that support allostasis. The seed coordinates are MNI X, Y, Z = 46, 12, 28. These results are from the discovery sample ($N$ = 280). Identical conclusions were obtained using results for the replication sample ($N$ = 270). The color scale ranges from $p = 0.05$ in red to $p = 10^{-50}$ in yellow, uncorrected and on a log scale. PAG = periaqueductal gray; PBN = parabrachial nucleus; V. Striatum = ventral striatum; NTS = nucleus of the solitary tract.

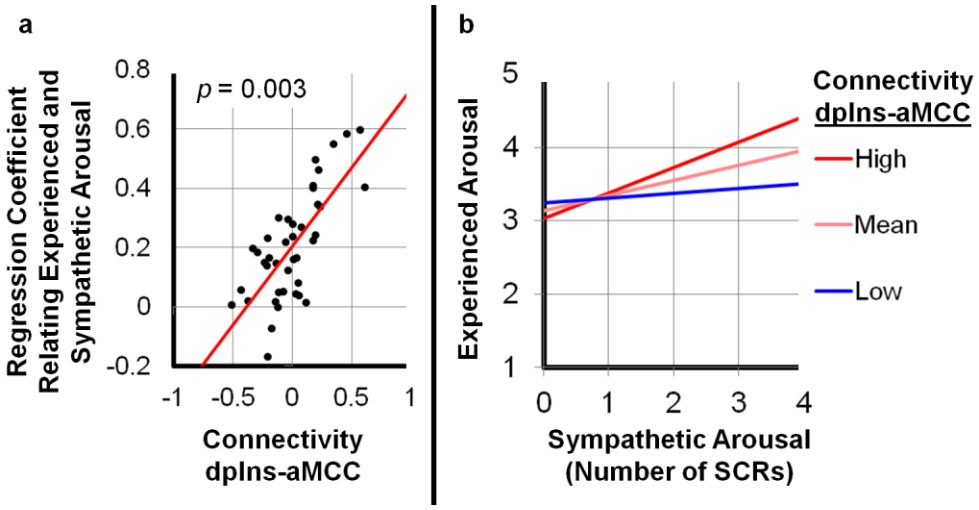


**Supplementary Figure 8.** The strength of intrinsic connectivity within the allostatic/interoceptive system predicts the degree of interoception during allostatic fluctuations. (a) Each data point corresponds to one participant ($N$ = 41). Interoceptive ability is represented on the y-axis as the unstandardized linear regression coefficient $B$ for the relationship between sympathetic nervous system arousal (i.e., the number of skin conductance responses) and the intensity of experienced arousal (rated on a 1 to 5 scale) while participants viewed evocative pictures. The strength of intrinsic connectivity between a primary interoceptive region (dorsal posterior insula, or dpIns) and a key visceromotor control region (the anterior portion of the midcingulate cortex, or aMCC) is represented on the x-axis as the Fisher's z transformation of the Pearson's correlation coefficient of the two BOLD time courses (the red line shows the regression line with coefficient $B$ = 0.56; $p$ = 0.003; multi-level regression analysis). (b) The relationship between experienced arousal and the number of skin conductance responses (as an index of sympathetic nervous system arousal) is moderated by intrinsic connectivity strength. "High" or "Low" corresponds to one SD above or below the mean connectivity across participants, respectively (mean 0.1, SD 0.23). dpIns = dorsal posterior insula; aMCC = anterior midcingulate cortex; SCRs = skin conductance responses.

**Supplementary References**


1 Craig, A. D. How do you feel? Interoception: The sense of the physiological condition of the body. *Nature reviews. Neuroscience* **3**, 655-666 (2002).

2 Nieuwenhuys, R., Voogd, J. & Huijzen, C. v. in *The human central nervous system* Ch. 8, 253-279 (Springer, 2008).

3 Nieuwenhuys, R., Voogd, J. & Huijzen, C. v. in *The human central nervous system* Ch. 10, 289-336 (Springer, 2008).

4 Ongur, D., An, X. & Price, J. L. Prefrontal cortical projections to the hypothalamus in macaque monkeys. *J. Comp. Neurol.* **401**, 480-505 (1998).

5 Mufson, E. J., Mesulam, M. M. & Pandya, D. N. Insular interconnections with the amygdala in rhesus monkey. *Neuroscience* **6**, 1231-1248 (1981).

6 Rempel-Clower, N. L. & Barbas, H. Topographic organization of connections between the hypothalamus and prefrontal cortex in the rhesus monkey. *J. Comp. Neurol.* **398**, 393-419 (1998).

7 Freedman, L. J., Insel, T. R. & Smith, Y. Subcortical projections of area 25 (subgenual cortex) of the macaque monkey. *J. Comp. Neurol.* **421**, 172-188 (2000).

8 Cavdar, S. *et al.* The afferent connections of the posterior hypothalamic nucleus in the rat using horseradish peroxidase. *J. Anat.* **198**, 463-472 (2001).

9 Ongur, D., Ferry, A. T. & Price, J. L. Architectonic subdivision of the human orbital and medial prefrontal cortex. *J. Comp. Neurol.* **460**, 425-449 (2003).

10 Ongur, D. & Price, J. L. The organization of networks within the orbital and medial prefrontal cortex of rats, monkeys and humans. *Cereb. Cortex* **10**, 206-219 (2000).

11 Pisotta, I. & Molinari, M. Cerebellar contribution to feedforward control of locomotion. *Front. Hum. Neurosci.* **8**, 475 (2014).

12 Wolpert, D. M. & Kawato, M. Multiple paired forward and inverse models for motor control. *Neural Netw* **11**, 1317-1329 (1998).

13 Buckner, R. L., Krienen, F. M., Castellanos, A., Diaz, J. C. & Yeo, B. T. The organization of the human cerebellum estimated by intrinsic functional connectivity. *J. Neurophysiol.* **106**, 2322-2345 (2011).

14 Nieuwenhuys, R., Voogd, J. & Van Huijzen, C. in *The human central nervous system* Ch. 13, 401-426 (Springer, 2008).

15 Seeley, W. W. *et al.* Dissociable intrinsic connectivity networks for salience processing and executive control. *J. Neurosci.* **27**, 2349-2356 (2007).

16 Raichle, M. E. The brain's default mode network. *Annu. Rev. Neurosci.* **38**, 433-447 (2015).

17 Hoistad, M. & Barbas, H. Sequence of information processing for emotions through pathways linking temporal and insular cortices with the amygdala. *Neuroimage* **40**, 1016-1033 (2008).

18 Mesulam, M. M. & Mufson, E. J. Insula of the old world monkey. Iii: Efferent cortical output and comments on function. *J. Comp. Neurol.* **212**, 38-52 (1982).

19 Aggleton, J. P., Burton, M. J. & Passingham, R. E. Cortical and subcortical afferents to the amygdala of the rhesus monkey (macaca mulatta). *Brain Res.* **190**, 347-368 (1980).

20 Stefanacci, L. & Amaral, D. G. Some observations on cortical inputs to the macaque monkey amygdala: An anterograde tracing study. *J. Comp. Neurol.* **451**, 301-323 (2002).

21 Ghashghaei, H. T., Hilgetag, C. C. & Barbas, H. Sequence of information processing for emotions based on the anatomic dialogue between prefrontal cortex and amygdala. *Neuroimage* **34**, 905-923 (2007).

22 Nieuwenhuys, R., Voogd, J. & Van Huijzen, C. in *The human central nervous system* Ch. 12, 361-400 (Springer, 2008).

23 Haber, S. N. & Behrens, T. E. The neural network underlying incentive-based learning: Implications for interpreting circuit disruptions in psychiatric disorders. *Neuron* **83**, 1019-1039 (2014).

24 Swanson, L. W. Cerebral hemisphere regulation of motivated behavior. *Brain Res.* **886**, 113-164 (2000).

25 Chikama, M., McFarland, N. R., Amaral, D. G. & Haber, S. N. Insular cortical projections to functional regions of the striatum correlate with cortical cytoarchitectonic organization in the primate. *J. Neurosci.* **17**, 9686-9705 (1997).

26 Room, P., Russchen, F. T., Groenewegen, H. J. & Lohman, A. H. Efferent connections of the prelimbic (area 32) and the infralimbic (area 25) cortices: An anterograde tracing study in the cat. *J. Comp. Neurol.* **242**, 40-55 (1985).

27 Price, J. L. & Amaral, D. G. An autoradiographic study of the projections of the central nucleus of the monkey amygdala. *J. Neurosci.* **1**, 1242-1259 (1981).

28 Haber, S. N., Kim, K. S., Mailly, P. & Calzavara, R. Reward-related cortical inputs define a large striatal region in primates that interface with associative cortical connections, providing a substrate for incentive-based learning. *J. Neurosci.* **26**, 8368-8376 (2006).

29 Fudge, J. L., Breitbart, M. A., Danish, M. & Pannoni, V. Insular and gustatory inputs to the caudal ventral striatum in primates. *J. Comp. Neurol.* **490**, 101-118 (2005).

30 Carrive, P. in *The human nervous system* (eds Mai J.K. & Paxinos G.) 367-400 (Academic Press, 2012).

31 Satpute, A. B. *et al.* Identification of discrete functional subregions of the human periaqueductal gray. *Proc. Natl. Acad. Sci. U. S. A.* **110**, 17101-17106 (2013).

32 An, X., Bandler, R., Ongur, D. & Price, J. L. Prefrontal cortical projections to longitudinal columns in the midbrain periaqueductal gray in macaque monkeys. *J. Comp. Neurol.* **401**, 455-479 (1998).

33 Paxinos, G., Feng-Xu, H., Sengul, G. & Watson, C. in *The human nervous system* (eds J. K. Mai & G. Paxinos) Ch. 8, 260-327 (Springer, 2012).

34 Saper, C. B. Reciprocal parabrachial-cortical connections in the rat. *Brain Res.* **242**, 33-40 (1982).

35 Saper, C. B. Convergence of autonomic and limbic connections in the insular cortex of the rat. *J. Comp. Neurol.* **210**, 163-173 (1982).

36 Vogt, B. A. & Palomero-Gallagher, N. in *The human central nervous system* (eds J.K. Mai & G. Paxinos) Ch. 25, 943-987 (Elsevier, 2012).

37 Craig, B. *How do you feel?: An interoceptive moment with your neurobiological self*. (Princeton University Press, 2014).

38 Damasio, A. & Carvalho, G. B. The nature of feelings: Evolutionary and neurobiological origins. *Nat. Rev. Neurosci.* **14**, 143-152 (2013).

39 Critchley, H. D. & Harrison, N. A. Visceral influences on brain and behavior. *Neuron* **77**, 624-638 (2013).

40 Terreberry, R. R. & Neafsey, E. J. Rat medial frontal cortex: A visceral motor region with a direct projection to the solitary nucleus. *Brain Res.* **278**, 245-249 (1983).

41 van der Kooy, D., McGinty, J. F., Koda, L. Y., Gerfen, C. R. & Bloom, F. E. Visceral cortex: A direct connection from prefrontal cortex to the solitary nucleus in rat. *Neurosci. Lett.* **33**, 123-127 (1982).

42 Dawson, M. E., Schell, A. M. & Filion, D. L. in *Handbook of psychophysiology* (eds J. T. Cacioppo, L. G. Tassinary, & G. G. Berntson) 159-181 (Cambridge University Press, 2007).

43 Bradley, M. M. & Lang, P. J. Measuring emotion: The self-assessment manikin and the semantic differential. *Journal of behavior therapy and experimental psychiatry* **25**, 49-59 (1994).

44 Peugh, J. L. A practical guide to multilevel modeling. *J. Sch. Psychol.* **48**, 85-112 (2010).

45 Bradley, M. M. & Lang, P. J. in *Handbook of emotion elicitation and assessment. Series in affective science* Vol. viii (eds J. A. Coan & J. J. B. Allen) (Oxford University Press, 2007).

46 van den Heuvel, M. P. & Sporns, O. Rich-club organization of the human connectome. *J. Neurosci.* **31**, 15775-15786 (2011).

47 Murphy, K., Birn, R. M., Handwerker, D. A., Jones, T. B. & Bandettini, P. A. The impact of global signal regression on resting state correlations: Are anti-correlated networks introduced? *Neuroimage* **44**, 893-905 (2009).

48 Yeo, B. T. *et al.* The organization of the human cerebral cortex estimated by intrinsic functional connectivity. *J. Neurophysiol.* **106**, 1125-1165 (2011).

49 Risold, P. Y., Thompson, R. H. & Swanson, L. W. The structural organization of connections between hypothalamus and cerebral cortex. *Brain Res. Brain Res. Rev.* **24**, 197-254 (1997).

50 Parvizi, J., Van Hoesen, G. W., Buckwalter, J. & Damasio, A. Neural connections of the posteromedial cortex in the macaque. *Proc. Natl. Acad. Sci. U. S. A.* **103**, 1563-1568 (2006).

51 Dujardin, E. & Jurgens, U. Afferents of vocalization-controlling periaqueductal regions in the squirrel monkey. *Brain Res.* **1034**, 114-131 (2005).

52 Saper, C. B. in *The human nervous system* (eds J. K. Mai & G. Paxinos) Ch. 16, 548-583 (Elsevier, 2012).

53 Lang, P. J., Bradley, M. M. & Cuthbert, B. N. International affective picture system (iaps): Affective ratings of pictures and instruction manual. *Technical Report A-8. University of Florida, Gainesville, FL.* (2008).

54 van den Heuvel, M. P. & Sporns, O. An anatomical substrate for integration among functional networks in human cortex. *J. Neurosci.* **33**, 14489-14500 (2013).

55 Bickart, K. C. *et al.* Atrophy in distinct corticolimbic networks in frontotemporal dementia relates to social impairments measured using the social impairment rating scale. *J. Neurol. Neurosurg. Psychiatry* **85**, 438-448 (2014).

56 Touroutoglou, A., Andreano, J. M., Barrett, L. F. & Dickerson, B. C. Brain network connectivity-behavioral relationships exhibit trait-like properties: Evidence from hippocampal connectivity and memory. *Hippocampus* (2015).